Electronic Supplementary Information (ESI)

Fig. S1 XRD patterns of the CdS-N and the noble metal (Pt, Ru, or Pd)-modified CdS-N prepared by the OPS method.
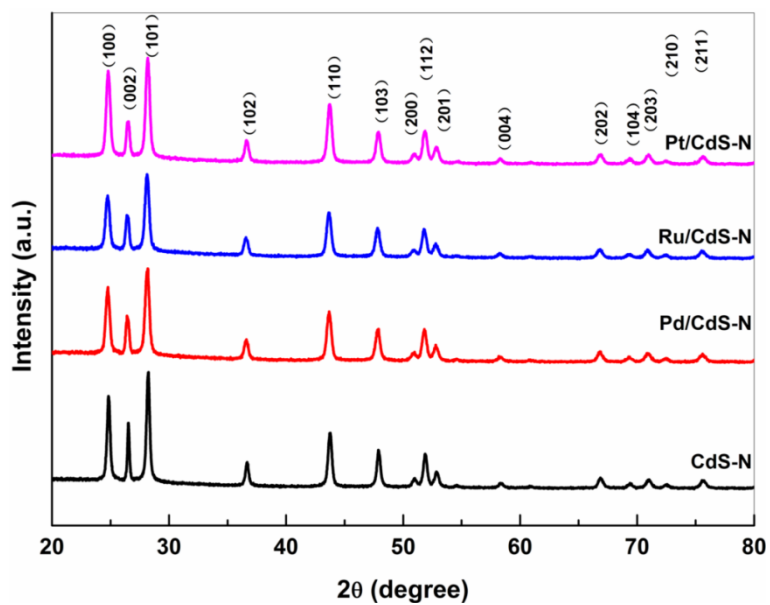

Fig. S1 indicates the noble metal (Pt, Ru, or Pd)-modified CdS-N shows identical diffraction pattern to the pristine CdS-N. All the diffraction peaks can be indexed to the hexagonal phase CdS and no peak originates from the noble metal can be perceived.

Fig. S2 UV-vis DRS spectra of CdS-N and the noble metal (Pt, Ru, or Pd)-modified CdS-N prepared by the OPS method.
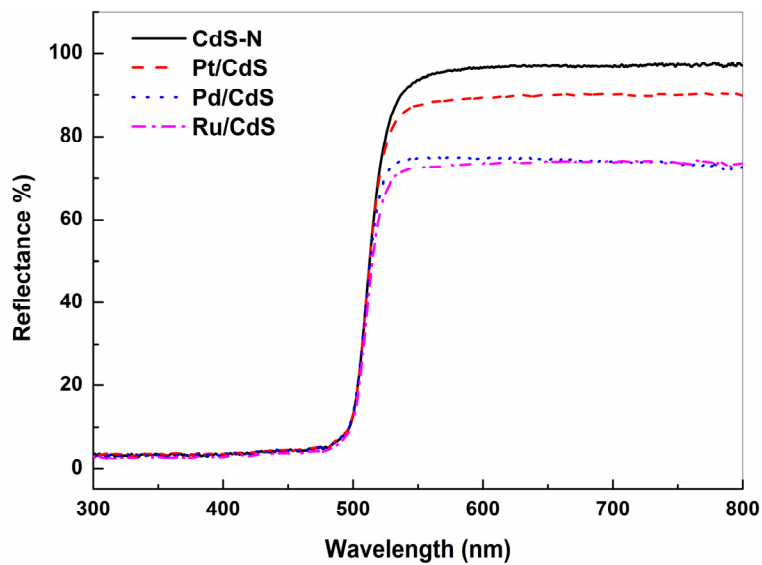

Fig. S2 indicates the noble metal (Pt, Ru, or Pd)-modified CdS-N show a same band gap absorption as that of pristine CdS-N. But, due to the presence of the noble metal, the absorption in visible light range is slightly improved.

Fig. S3 (a) TEM image of Pt/CdS-N, and SEM images of the prepared (b) Pt/CdS-N, and (c) Pt/CdS-P.
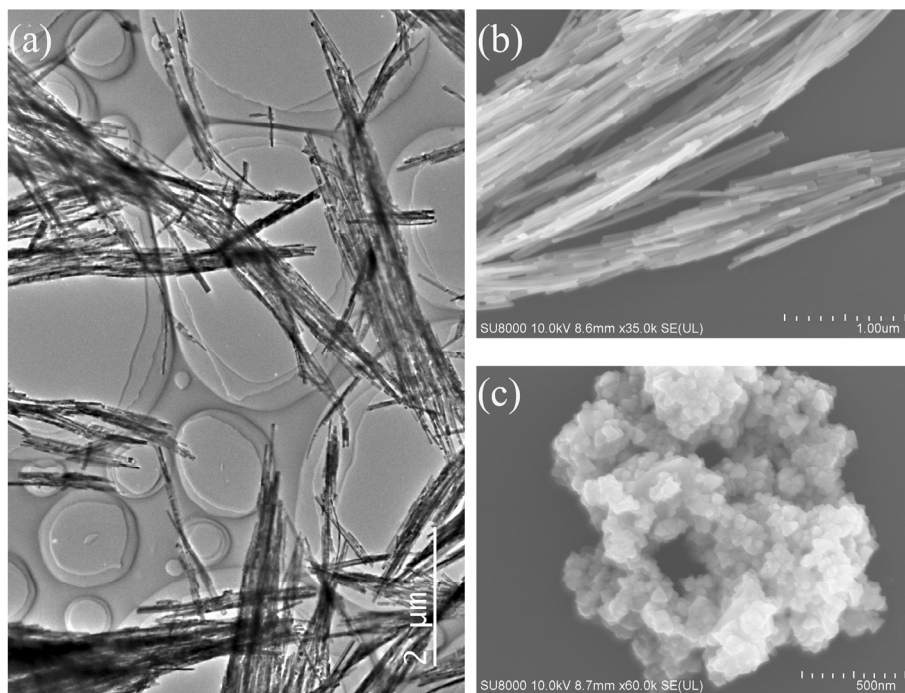

Fig. S3-a demonstrates the length of the prepared CdS nanorods is in the range of 1-6 μm. The smooth surface feature of Pt/CdS-N is further confirmed by the SEM image (Fig. S3-b). Fig. S3-c indicates the sample is composed by nanoparticles with no distinctive morphology. The average size of the particles is ca. 100 nm.

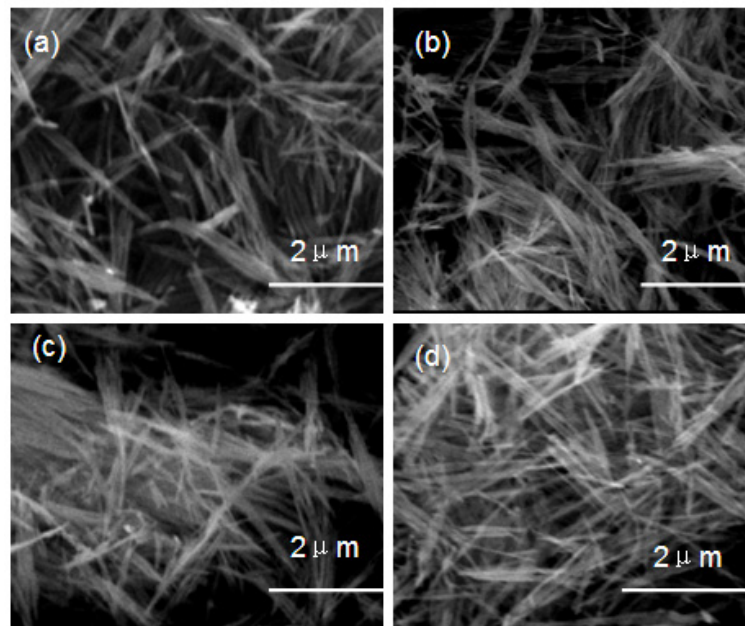Fig. S4 SEM images of the prepared (a) CdS-N, (b) Ru/CdS-N, (c) Pt/CdS-N(c), and (d) Pd/CdS-N.

Fig. S4 indicates the morphology of CdS-N sample is not affected by the deposition of noble metals. M/CdS-N (M=Pt, Pd, Ru) samples maintains a rod-like structure.

Fig. S5 Nitrogen adsorption-desorption isotherms of the CdS-N, CdS-P, and the corresponding platinized samples prepared by the OPS method. Inset shows the corresponding BET transform plots of 1/Q [(P$_0$/P)-1] versus P/P$_0$.
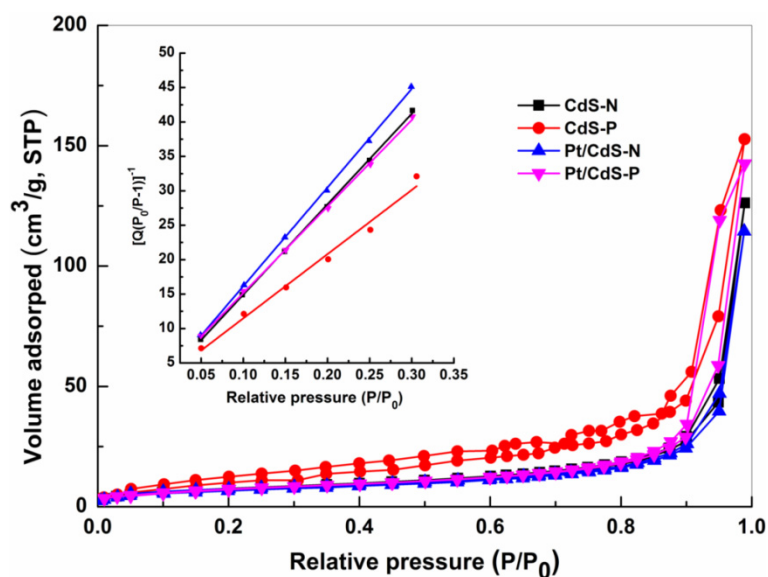
As shown in Fig. S5, the N$_2$ adsorption-desorption curves are of a type V isotherm with a H3 type of hysteretic loop. A disordered mesoporous structure formed by the agglomeration of small particles, therefore, can be expected in these samples. Based on the N$_2$ isotherm data, the BET surface area of PT samples can be derived. The linear fits to the corresponding BET transform plot of 1/Q[(P$_0$/P)-1] versus P/P$_0$ (where Q is the quantity of adsorbed N$_2$ (cm^3/g, STP), P/P$_0$<0.3) are shown in the inset of Fig. S5. The BET results derived from the linear fits are listed in Tab. 1. The surface area of CdS-P (36 m$^2\cdot$g^{-1}) is larger than that of CdS-N (26 m$^2\cdot$g^{-1}). A decrease of the surface areas can be observed after deposition of Pt, Pd, or Ru.

Fig. S6 UV-vis DRS spectra of the CdS-N samples loaded with different amount of Pt. The samples were prepared by the OPS method.
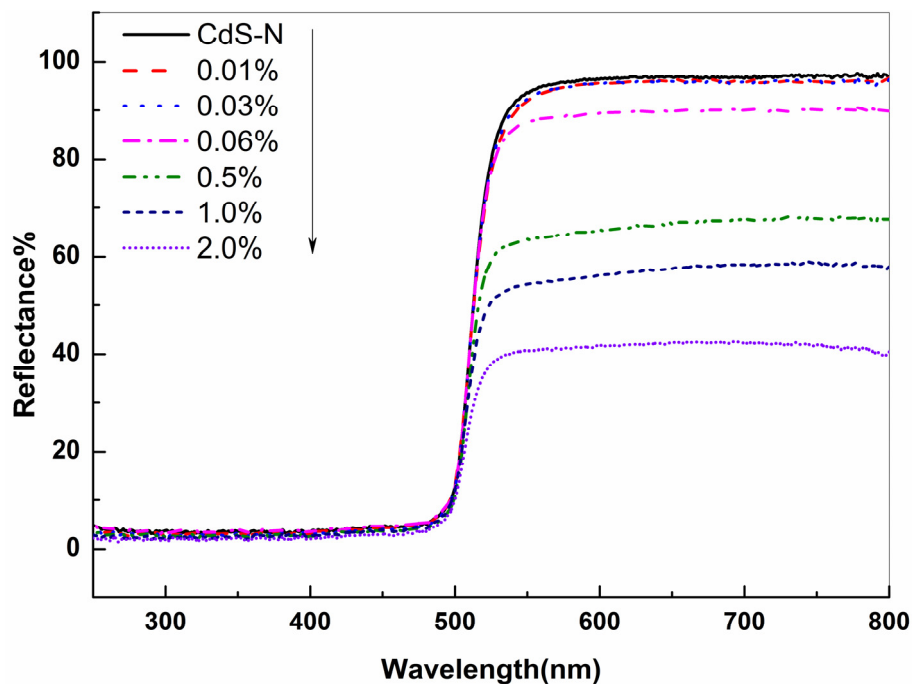

Fig. S6 indicates the visible absorption efficient of the platinized CdS-N increases with Pt amount. This absorption caused by the deposited Pt. The absorption of CdS will be reduced by the excessive Pt due to its shielding effect.

Table S1 Comparison the photocatalytic H_2 production activity of CdS based photocatalysts over lactic acid solution.

| Entry | Photocat. | Co-cat. & amount[a] | Preparation method | Reaction condition | | | r_{H2}[b] | r'_{H2}[c] | Ref |
				Light source	Dosage (mg)	Solution (V.%)/(mL)			
1	CdS	0.2% MoS$_2$	Impregnation-sulfidation	300 W Xe-lamp, λ>420 nm	100	10%/200	0.54	5.4	[1]
2	CdS	0.9mol% MoS$_2$	Ball milled	300 W Xe-lamp, λ>420 nm	100	10%/150	1.31	13.1	[2]
3	CdS/RGO	1.5% MoS$_2$	Solvothermal	350 W Xe-lamp, λ>420 nm	50	10%/100	0.10	2.0	[3]
4	CdS/UIO-66	1.5% MoS$_2$	Solvothermal	300 W Xe-lamp, λ>420 nm	20	10%/80	0.65	32.5	[4]
5	CdS	2% MoS$_2$	Hydrothermal-calcination	300 W Xe-lamp, λ>400 nm	100	10%/100	0.41	4.1	[5]
6	CdS	2 % MoS$_2$	Sonication-mixing	300 W Xe-lamp, λ>420 nm	200	20%/300	2.59	13.0	[6]
7	CdS /GR	2 % MoS$_2$	hydrothermal	500W UV lamp, 280-320 nm	20	10%/100	0.14	7.0	[7]
8	CdS-GR	5% MoS$_2$	Hydrothermal	300 W Xe-lamp, λ>400 nm	100	20%/160	2.32	23.2	[8]
9	CdS	? % WS$_2$[d]	hot injection	300 W Xe-lamp, λ>420 nm	10	10%/10	0.02	2.0	[9]
10	CdS/ZnS	1% WS$_2$	Hydrothermal	300 W Xe-lamp, λ>420 nm	100	10%/150	0.78	7.8	[10]
11	CdS	1.0% WS$_2$	Impregnation-sulfidation	300 W Xe-lamp, λ>420 nm	100	10%/200	0.42	4.2	[11]
12	CdS	1.2mol% NiS	hydrothermal	300 W Xe-lamp, λ>420 nm	300	30%/100	2.18	7.3	[12]
13	CdS/GR	1.0% SiW$_{11}$Co	hydrothermal	300 W Xe-lamp, λ>400 nm	100	30/160	1.7	17.0	[13]
14	g-C$_3$N$_4$/CdS	5% Au	Calcination-deposition	300 W Xe-lamp, λ>420 nm	100	20%/80	0.11	1.1	[14]
15	CdS	0.1% Pt	Coprecipitation-annealing	300 W Xe-lamp, λ>400 nm	100	10%/?[d]	0.29	2.9	[15]
16	CdS	0.23% Pt	Solvothermal	350 W Xe-lamp, λ>420 nm	50	10%/80	1.21	24.2	[16]
17	CdS	0.36% Pt	Solvothermal	350 W Xe-lamp, λ>420 nm	50	10%/80	0.80	16.0	[17]
18	CdS	0.3% Pt	Solvothermal	350 W Xe-lamp, λ>420 nm	50	10%/80	1.49	29.8	[18]
19	CdS	0.5% Pt	Hydrothermal-sulfidation	350 W Xe-lamp, λ>420 nm	50	10%/80	0.47	9.4	[19]
20	CdS/RGO	0.5% Pt	Solvothermal	350 W Xe-lamp, λ>420 nm	20	10%/80	1.12	56.0	[20]

| Entry | Photocat. | Co-cat. & amount[a] | Preparation method | Reaction condition | | | r_{H2}[b] | r'_{H2}[c] | Ref |
				Light source	Dosage (mg)	Solution (V.%)/(mL)			
21	CdS	1% Pt$_3$Co	Hydrothermal	300 W Xe-lamp, λ>420 nm	10	10%/50	0.16	16.0	[21]
22	CdS/TiO$_2$	2% Pt	Hydrothermal-deposition	350 W Xe-lamp, λ>420 nm	40	10%/80	0.27	6.8	[22]
23	CdS QDs/GR	2.1% Pt	hot injection-sonication	300 W Xe-lamp, λ>420 nm	72	10%/100	2.15	29.9	[23]
24	CdS/WO$_3$	3% Pt	Hydrothermal	500 W Xe-lamp, λ>400 nm	50	?[d]	0.15	3.0	[24]
25	CdS	0.3% Pt	Solvothermal	300 W Xe-lamp, λ>400 nm	50	10%/100	0.81	16.2	This work
26	CdS	0.06% Pt	Solvothermal	300 W Xe-lamp, λ>400 nm	50	10%/100	0.51	10.2	This work

[a]: in wt.% term if unspecified; [b]: the highest evolution rate of H_2 (mmol·h^{-1}) obtained under the optimized condition; [c]: Specific rate, (mmol·g^{-1}·h^{-1}); [d] not given by the work.

References

(1)   (a) X. Zong, H. J. Yan, G. P. Wu, G. J. Ma, F. Y. Wen, L. Wang, C. Li. J. Am. Chem. Soc., 2008, 130, 7176. (b) X. Zong, G. Wu, H. Yan, G. Ma, J. Shi, F. Wen, L. Wang, C. Li. J. Phys. Chem. C, 2010, 114, 1963.

(2)   G. Chen, D. Li, F. Li, Y. Fan, H. Zhao, Y. Luo, R. Yu, Q. Meng. Appl. Catal. A Gen., 2012, 443-444, 138.

(3)   Y. Li, H. Wang, S. Peng. J. Phys. Chem. C, 2014, 118, 19842.

(4)   L. Shen, M. Luo, Y. Liu, R. Liang, F. Jing, L. Wu. Appl. Catal. B Environ., 2015, 166-167, 445.

(5)   J. Xu, X. Cao. Chem. Eng. J., 2015, 260, 642.

(6)   K. Chang, M. Li, T. Wang, S. Ouyang, P. Li, L. Liu, J. Ye. Adv. Energy Mater., 2015, 5.

(7)   T. T. Jia, A. Kolpin, C. S. Ma, R. C. T. Chan, W. M. Kwok, S. C. E. Tsang. Chem. Commun., 2014, 50, 1185.

(8)   M. Liu, F. Li, Z. Sun, L. Ma, L. Xu, Y. Wang. Chem. Commun., 2014, 50, 11004.

(9)   J. Chen, X. J. Wu, L. Yin, B. Li, X. Hong, Z. Fan, B. Chen, C. Xue, H. Zhang. Angew. Chem. Int. Ed., 2015, 54, 1210.

(10)   G. Chen, F. Li, Y. Fan, Y. Luo, D. Li, Q. Meng. Catal. Commun., 2013, 40, 51.

(11)   X. Zong, J. Han, G. Ma, H. Yan, G. Wu, C. Li. J. Phys. Chem. C, 2011, 115, 12202.

(12)   W. Zhang, Y. Wang, Z. Wang, Z. Zhong, R. Xu. Chem Commun, 2010, 46, 7631.

(13)   M. Liu, F. Li, Z. Sun, L. Xu, Y. Song, A. Munventwali. RSC Adv., 2015, 5, 47314.

(14)   W. Li, C. Feng, S. Dai, J. Yue, F. Hua, H. Hou. Appl. Catal. B Environ., 2015, 168-169, 465.

(15)   G. Xin, B. Yu, Y. Xia, T. Hu, L. Liu, C. Li. J. Phys. Chem. C, 2014, 118, 21928.

(16)   J. Yu, Y. Yu, B. Cheng. RSC Adv., 2012, 2, 11829.

(17)   J. Yu, Y. Yu, P. Zhou, W. Xiao, B. Cheng. Appl. Catal. B Environ., 2014, 156-157, 184.

(18)   J. Jin, J. Yu, G. Liu, P. K. Wong. J. Mater. Chem. A, 2013, 1, 10927.

(19)   Q. J. Xiang, B. Cheng, J. G. Yu. Appl. Catal. B Environ., 2013, 138, 299.

(20)   Q. Li, B. Guo, J. Yu, J. Ran, B. Zhang, H. Yan, J. R. Gong. J. Am. Chem. Soc., 2011, 133, 10878.

(21)   Z. F. Hu, J. C. Yu. J. Mater. Chem. A, 2013, 1, 12221.

(22)   L. Qi, J. Yu, M. Jaroniec. Phys. Chem. Chem. Phys., 2011, 13, 8915.

(23)   Z. Fang, Y. B. Wang, J. B. Song, Y. M. Sun, J. J. Zhou, R. Xu, H. W. Duan. Nanoscale, 2013, 5, 9830.

(24)   L. J. Zhang, S. Li, B. K. Liu, D. J. Wang, T. F. Xie. ACS Catal., 2014, 4, 3724.